Response to Referee #1:

We thank referee #1 for their helpful comments. Our responses are given below in black with the referee's comments in blue. The new text in the modified manuscript is given in red (italicized).

Referee #1:

General comments

This paper describes the process to obtain the surface NO2 mixing ratio using the NO2 column from the ground-based Pandora observation. Some validations are performed by the comparison to the model outputs and in-situ measurement. The approaches look logical and the final products seem reasonable. Considering the rising importance of Pandora data for the air quality monitoring, publication of this work is useful to the research community and potential readers. But some more discussions should be included to improve this manuscript. Please refer to the comments below for the revision process.

Specific comments

P1, L27: Traffic is one of the important NO2 sources. Please include.

Done.

It is primarily emitted from combustion processes such as fossil fuel combustion (e.g., traffic, electricity generation from power plants) and biomass burning, as well as from lightning. NO_2 is a nitrate aerosol precursor, and it also contributes to acid deposition and eutrophication (ECCC, 2016).

P2 L1-L12: Why is the total vertical column NO2 significantly treated first instead of insitu measurement. For air quality monitoring, in-situ measurement has been performed basically. Before the importance of Pandora observation is addressed, the necessity of ground-based remote sensing of trace gases should be stated first, in spite of the well-structured ground-based in-situ networks.

A new paragraph has been included in the Introduction to describe the current in situ measurements and the monitoring network (NAPS).

As surface NO_2 concentrations are regulated by many environmental agencies (e.g., Environment and Climate Change Canada and U.S. Environmental Protection Agency), in situ NO_2 measurements are commonly carried out by many national monitoring networks, such as the National Air Pollution Surveillance (NAPS, https://www.canada.ca/en/environment-climate-change/services/air-pollution/monitoring-networks-data/national-air-pollution-program.html) network in Canada, which was established in 1969. The in situ methods used to measure surface NO_2 have evolved over the years; for example, luminol chemiluminescence (e.g., Kelly et al., 1990; Maeda et al., 1980; Wendel et al., 1983), long-path differential optical absorption spectroscopy (e.g., Platt, 1994), photolytic *conversion/chemiluminescence (e.g., Gao et al., 1994; Ryerson et al., 2000), and laser-induced fluorescence (e.g., Thornton et al., 2000) are all found to be reliable methods with an uncertainty within 10 % at the 1 ppbv and higher concentration levels (McClenny, 2000). Currently, the in situ approach used by NAPS for surface NO_2 air quality monitoring is the photolytic conversion/chemiluminescence technique, which converts NO_2 to NO and subsequently detects the NO by chemiluminescence reaction (McClenny, 2000; NRC, 1992). This in situ monitoring provides good measurements at ground level (0.4 ppbv accuracy), but NO_2 is not uniformly mixed through the atmosphere, and not even within the atmospheric boundary layer due to emission and removal processes taking place at the surface.*

P2 L8-9: The reason to use zenith-sky observations under the cloudy condition is not clear. Why zenith sky mode has more reliable than direct-sun mode under the cloudy condition?

The direct-sun mode requires unobscured sun to make reliable measurements. We have modified the text as follows:

Zenith-sky observations have been widely used for stratospheric ozone and NO_2 observations, particularly under cloudy conditions when direct-sun measurements are unreliable (note that zenith-sky observations use scattered sunlight and are less sensitive to clouds, e.g., Zhao et al. (2019)).

P4 L20-21: Why do we need O4 retrieval? Still, some potential readers do not have any idea about the meaning of O4 retrieval.

Some background information about O_4 is included in this new paragraph.

The oxygen collision complex $(O_2)_2$ (referred here as O_4), which is created by the collision of two oxygen molecules, has broadband absorptions from UV to near IR spectral ranges (Greenblatt et al., 1990; Platt and Stutz, 2008; Thalman and Volkamer, 2013). O_4 is widely used as a reference gas by many DOAS applications to infer cloud and aerosol properties (e.g., Gielen et al., 2014; Wagner et al., 2004, 2014, 2016; Wang et al., 2015; Zhao et al., 2019).

P7 L1-2: In other Pandora paper (usually including Dr. Jay Herman in the author list), diurnal variation of stratospheric NO2 is not much considered. It will be more interesting (and even useful) to add some arguments compared with their approaches.

In short, there are two major concepts we must consider here, 1) the NO_2 profile (weights between stratospheric and tropospheric NO_2), and 2) the observation geometry (direct-sun or zenith-sky).

To calculate proper AMFs, there are two things that must be considered: the day-night difference due to photochemistry and the morning and evening peaks of NO_2 due to local traffic. As discussed in the paper (see Fig. A1b), the stratospheric diurnal variation contributes about 0.1 DU difference in total column NO_2. Thus, this amount is large enough to matter for urban sites such as Toronto, and can be more significant for rural sites. In general, our conclusion is that an urban site with direct-sun observation should have smaller impact from the stratospheric diurnal variation. On the other hand, a rural site with zenith-sky observation should have a significant impact. This information has now been included in Appendix B as follows:

Please note that the strength of this bias is related to 1) the NO_2 profile (weights between stratospheric and tropospheric NO_2), and 2) the observation geometry (direct-sun or zenith-sky). In general, an urban site with direct-sun observation should have smaller impact from the stratospheric diurnal variation. On the other hand, a rural site with zenith-sky observation should have significant impact.

P8 L10-24: Notation is not clear. There are VCD_DS and VCE_ZS. Also, there are VCD_EMP and VCD_NDACC. VCD_EMP (and VCD_NDACC) is related to VCD_DS or VCD_ZS? Better notation or more description of these notations look required.

VCD_{EMP} and VCD_{NDACC} are both VCDs retrieved from zenith-sky observations. To make our notation clearer, we have changed VCD_{EMP} and VCD_{NDACC} to $VCD_{ZS\text{-}EMP}$ and $VCD_{ZS\text{-}NADCC}$. The corresponding text has been changed as follows:

Total column NO_2 can then be retrieved using Eqn. (1) and these two sets of AMFs, where the one based on empirical AMFs is referred to as $VCD_{ZS\text{-}Emp}$ and the one based on NDACC AMFs is referred to as $VCD_{ZS\text{-}NDACC}$. The RCD value used in the retrievals is 0.39 ± 0.01 DU, which is retrieved along with $AMF_{ZS\text{-}Emp}$ (Appendix A).

In general, the $VCD_{ZS\text{-}Emp}$ and $VCD_{ZS\text{-}NDACC}$ performed as expected. Compared with VCD_{DS}, the $VCD_{ZS\text{-}NDACC}$ shows a -25% bias, while the $VCD_{ZS\text{-}Emp}$ only shows a -4 % bias (indicated by the red lines on each panel and their slopes). In addition, $VCD_{ZS\text{-}Emp}$ shows less SZA dependence than $VCD_{ZS\text{-}NDACC}$ (see the increased bias for measurements made in larger SZA conditions in Figure 2b).

P10 L10-12: V_ftrop is from the GEOS-chem simulations. How does GEOS-Chem consider the lightning NOx in the free-troposphere? In other words, GEOS-Chem can catch the free-tropospheric lightening NOx reasonably? It seems better to include some discussions about the estimation of lightning NOx in the free troposphere and even stratosphere, which is related to the final quality of C_pan from the Pandora observation.

Lightning NO_x emissions are computed as a function of cloud-top height, and are scaled globally as described by Sauvage et al. (2007) to match Optical Transient Detector/Lightning Imaging Sensor (OTD/LIS) climatological observations of lightning flashes. The global source is imposed to be 6 Tg(N) yr^{-1}

(Martin et al., 2007). Higher NO_x yields per flashes are used at mid-latitudes than in the tropics (Hudman et al., 2007). Different versions of the GEOS-CHEM model have been used extensively in the retrieval of tropospheric VCDs, and have been shown capable of simulating the vertical distributions of NO_2 (e.g. Lamsal et al., 2008; Martin et al., 2002) and SO_2 (e.g. Lee et al., 2009). Some of this information about the estimation of lightning NOx has now been included in Section 2.2.2.

The model has a detailed representation of tropospheric chemistry, including aerosols and their precursors (Park et al., 2004). In the simulation used in this study, a global lightning NO_x source of 6 Tg N yr^{-1} (Martin et al., 2002) was imposed. Lightning NO_x emissions are computed as a function of cloud-top height, and are scaled globally as described by Sauvage et al. (2007) to match Optical Transient Detector/Lightning Imaging Sensor (OTD/LIS) climatological observations of lightning flashes.

To provide some quality information about the final data product (C_{Pan}), a detailed uncertainty estimation has been provided in a new Appendix D. In general, the contribution from the free tropospheric NO_2 is limited compared to lower tropospheric and stratospheric NO_2, as suggested by the following paragraph from Appendix D:

The estimated Pandora zenith-sky-based surface NO_2 data have uncertainties from 4.8 to 6.5 ppbv. In Eqn. 8, the contributions of the V_{Pan}, V_{Strat}, V_{ftrop}, and R_{CV} terms to the total uncertainty are 36%, 2%, 0.3%, and 62 %, respectively. This result indicates that the uncertainty in the Pandora zenith-sky-based surface NO_2 is dominated by the uncertainties of Pandora zenith-sky total column NO_2 and modelled column-to-surface conversion ratio (R_{CV}). However, please note that this uncertainty budget depends on the NO_2 vertical distributions, and may vary from site to site; e.g., in Toronto, the tropospheric NO_2 is typically 2-4 times higher than the stratospheric NO_2, and thus, the contribution to uncertainty from V_{Pan} is much larger than the corresponding contributions from V_{Strat} and V_{ftrop}.

P10 L22-24: How about the year-to-year variation of conversion ratio? Is it larger or smaller than the diurnal variation of conversion ratio? If there is, it seems to include some discussion for how to treat or consider the year-to-year variation.

A year-to-year variation of conversion ratio is expected. However, the magnitude of this variation depends on the conditions of the site (e.g., local emission patterns, year round sunlight period). In other words, as the ratio in the look-up table is calculated using monthly mean (data period: April 2016 to December 2017), it is expected that for different period, this ratio will be different. For example, if the local emission patterns or meteorological conditions have significant changes for a site, the derived conversion ratio should reveal these changes. In general, the look-up table approach ($C_{pan\text{-}LUT}$) is aiming for a quick and near-real-time data delivery. Thus, for a given year, we recommend using a mean PSC-LUT that is calculated from model simulations of previous years. On the other hand, for the off-line data, the $C_{pan\text{-}model}$ is the final, high-quality, year-specific data product that will be delivered to users. This information has now been included in this section:

In general, the look-up table approach ($C_{pan-LUT}$) is aiming for a quick and near-real-time data delivery. Thus, to minimize year-to-year variation (e.g., from changing meteorological conditions or changing local emission patterns), for a given year we recommend using a mean PSC-LUT that is calculated from model simulations of previous years. On the other hand, the $C_{pan-model}$ is the off-line, high-quality, year-specific data product that will be delivered for air quality research and other applications.

P11 L21-28: How to connect the results and discussions here to those in Fig. 4? The lesson from Fig. 4 seems that the ZS Pandora NO2 has better quality than the direct-sun Pandora NO2, right? But here both ZS and direct-sun Pandora NO2 shows consistent quality. Then what do we really learn from Fig. 4 in this work?

Please note the results in Fig. 4 are for total column NO_2, while the discussion in page 11 is about Pandora derived surface NO_2 concentrations. We also found slightly better agreement in Fig. 4 between Pandora zenith-sky NO_2 VCD with OMI. However, due to the limited number of coincident data, we think the zenith-sky and direct-sun Pandora NO_2 are of similar good quality. To further assess the quality, we need a longer period of observation and more coincident measurements. Some possible explanations are now included in Section 3.2.

The better correlation and lower bias for zenith-sky versus direct-sun might be a case of coincident errors, i.e., compare to Pandora direct-sun total column NO_2, both OMI and Pandora zenith-sky total column NO_2 underestimate the local NO_2 at Toronto (see Figure 2). When taking into account the standard error of the fitting and the confidence level of R, the difference between zenith-sky and direct-sun data is not significant (i.e, in Fig. 4 from panels a to d, the slopes with standard error are 0.64 ± 0.02, 0.67 ± 0.02, 0.70 ± 0.04, and 0.71 ± 0.03; the 95% confidence intervals for R values are 0.45 to 0.63, 0.61 to 0.75, 0.43 to 0.77, and 0.60 to 0.86).

P12 L3-18 and Fig. 8: In this study, the validation is performed for the 2015-2017 period. Why only a month (APR 2017) is considered in this analysis? The better quality of ZS NO2 than direct-sun NO2 can be justified with this figure but whether the ZS NO2 always provide the reliable NO2 under the heavy clouds cannot be determined based on only 1-month situation. It seems necessary to deal with additional cloudy cases (at least in the supplements).

Fig. 8 is an example of the time series. It was chosen because of its good mixture of clear, moderate cloud, and heavy cloud conditions. The general performance of cloud filtering was included in Appendix C, which examines the quality of ZS NO_2 in different cloud conditions (categorized by the enhancement of O_4) for the period April 2016 to December 2017. We have included another month (October 2016) with good mixed conditions in Appendix C as another example.

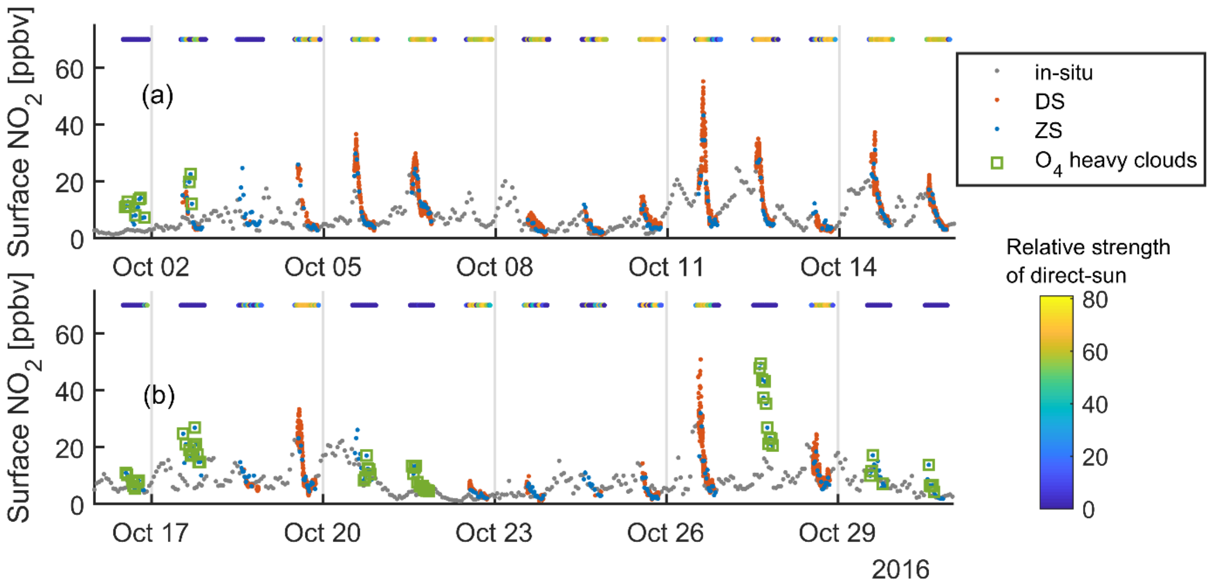

Figure A4. Example of surface NO_2 concentration time series in all conditions. The in situ, Pandora direct-sun (DS), and Pandora zenith-sky (ZS) surface NO_2 concentrations are shown by different coloured dots. The total sky imager relative strength of direct-sun data are plotted as a colour-coded horizontal dot-line on the top area of each panel. For Pandora zenith-sky data, the measurements with enhanced O_4 (heavy cloud indicator) are also labelled by green squares.

P13 L3-L20 and Figs. 9 and 10: In addition to the GEM-MACH model results, Pandora ZS and direct-sun NO2 products also show the higher standard deviation after sunrise compared to the time close to sunset. Considering the radiative extinction is more disturbed during the time close to sunrise and sunset, the higher standard deviation in the morning is not well understood. Why NO2 product in the morning has higher biases? This is also due to the propagation of GEM-MACH PBL uncertainty? (But authors mentioned that the surface NO2 from ZS Pandora observation is less dependent on the PBL height in P13 L29-30).

The standard deviations of Pandora ZS and DS in the morning are comparable to those of the in situ data. In Fig. 9, at 7:00 LST., in situ NO_2 is 14.9 ± 9.3 ppbv, while GEM-MACH, Pandora DS, and Pandora ZS NO_2 are 23.5 ± 15.0 ppbv, 15.6 ± 10.5 ppbv, and 15.2 ± 6.8 ppbv, respectively. To make it more clear, the shaded areas, which represent the 1σ envelope, have been modified to use dashed lines as boundaries.

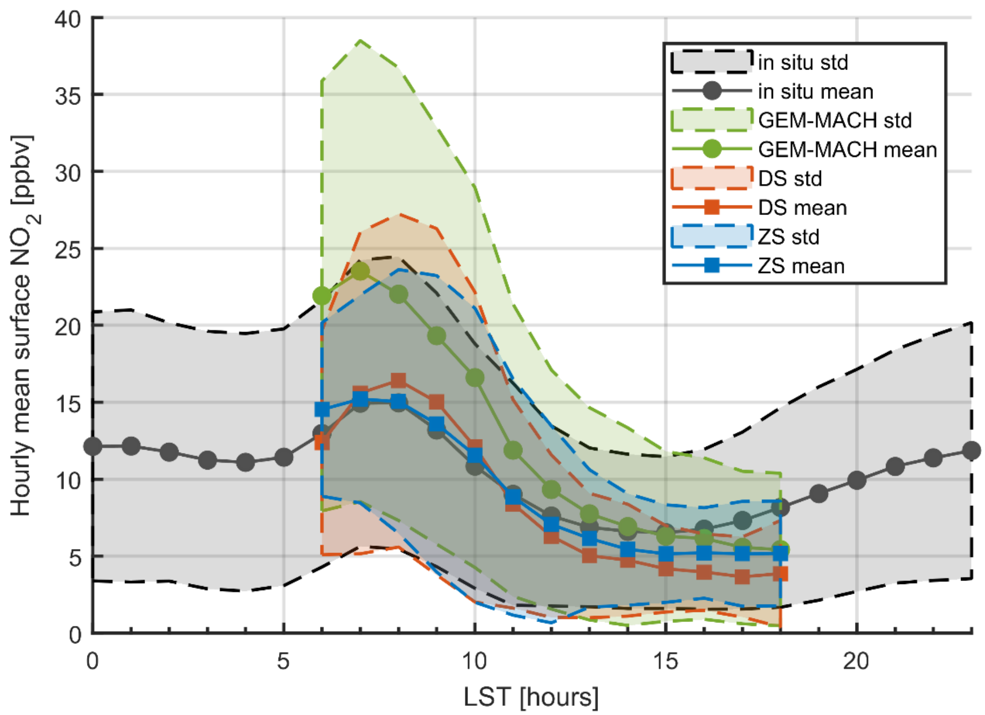

For evening conditions, in Fig. 9, at 17:00 LST, in situ NO_2 is 7.3 ± 5.8 ppbv, while GEM-MACH, Pandora DS, and Pandora ZS NO_2 are 5.6 ± 5.0 ppbv, 3.6 ± 2.6 ppbv, and 5.2 ± 3.4 ppbv, respectively. The larger morning standard deviations in all observations and modelled data are related to different NO_2 emission patterns in the mornings (i.e., work-days and weekend). The lower PBL in the mornings also enhanced the impacts from emissions compared to afternoon conditions. This information has now been included in the paragraph:

For example, at 7:00 LST, in situ NO_2 is 14.9 ± 9.3 ppbv, while GEM-MACH, Pandora DS, and Pandra ZS NO_2 are 23.5 ± 15.0 ppbv, 15.6 ± 10.5 ppbv, and 15.2 ± 6.8 ppbv, respectively. At 17:00 LST, in situ NO_2 is 7.3 ± 5.8 ppbv, while GEM-MACH, Pandora DS, and Pandora ZS NO_2 are 5.6 ± 5.0 ppbv, 3.6 ± 2.6 ppbv, and 5.2 ± 3.4 ppbv, respectively. The larger standard deviations in the morning are due to the datasets not being divided into work-days and weekends.

Technical corrections

P6 L2: two times -> twice

Done.

P7 L30-32: The meaning of this statement is not clear to me. Please more clarify the explanation.

It has been modified to be clearer.

Instead of finding the link between zenith-sky spectral intensity and total column values (i.e., following the Brewer and Dobson zenith-sky total ozone retrieval method), deriving empirical zenith-sky AMFs for Pandora zenith-sky measurements is more straightforward since Pandora zenith-sky spectra can be analyzed to produce NO_2 dSCDs.

P8 L10-12: This statement looks redundant, just a repetition of statements above.

The statement in P8 L10-12 is not redundant. The notation of this part has been modified to make this clearer:

If we make an assumption that the coincident direct-sun (DS) and zenith-sky (ZS) measurements sampled the same air mass, then the empirical zenith-sky AMFs (referred to here as $AMF_{ZS\text{-}Emp}$) can be calculated by assuming $VCD_{DS} = VCD_{ZS}$, which gives

$$VCD_{DS}(SZA) = \frac{dSCD_{ZS}(SZA)+RCD_{ZS}}{AMF_{ZS-Emp}(SZA)}. \quad (2)$$

Next, we can use nearly-coincident VCD_{DS} and $dSCD_{ZS}$ in a multi-non-linear regression to retrieve $AMF_{ZS\text{-}Emp}$ and RCD_{ZS} together. To ensure the quality of the retrieved $AMF_{ZS\text{-}Emp}$, only high quality direct-sun total column NO_2 data are used with SZA < 75°. Details about the empirical zenith-sky AMF calculation are shown in Appendix A.

Figure 1 shows a comparison of the empirical zenith-sky AMFs and NDACC AMFs (calculated for the Toronto measurements). Total column NO_2 can then be retrieved using Eqn. (1) and these two sets of AMFs, where the one based on empirical AMFs is referred to as $VCD_{ZS\text{-}Emp}$ and the one based on NDACC AMFs is referred to as $VCD_{ZS\text{-}NDACC}$. The RCD value used in the retrievals is 0.39 ± 0.01 DU, which is retrieved along with $AMF_{ZS\text{-}Emp}$ (Appendix A).

P11 L10: This result (slightly lower correlation) -> This slightly lower correlation Figs. 4, 7, and A2: If a slope value is the only significant value, then 'slope = ***' looks better expression. If authors would show the information with the format of 'y = slope x', it seems better to add intercept values together, to have the original regression equation (the equation looks not completed without intercept values)

The fitting that we used here is not a simple linear fitting, but a non-linear fit with intercept set to zero (this information was provided in the captions of Figs. 4, 7, and A2). The reason to force the intercept to be zero is to provide a meaningful value to represent the bias between two datasets. The assumption we made here is that if atmospheric NO_2 is zero, then any instrument should measure zero NO_2. In other words, the assumption is that there should be no additive systematic bias between instruments (i.e., drifting from zero), but only multiplicative systematic bias exist. In reality, although this assumption might not be true, for any instrument that we know, if it has a drift from zero (an additive systematic bias) we first correct this drifting before using its data. In other words, although the intercept value in simple linear fitting could be an indicator for multiplicative systematic bias between instruments, the value itself depends on which instrument we trust as truth (i.e., which dataset is used as y, and which dataset is used as x). Thus, the intercept is not really a meaningful indicator to show here.

In short, the fittings (intercept forced to be zero) are used to reveal the bias between two datasets, and the equations shown on those figures are complete.

Figure captions: It seems that all figure captions can be more clarified to better describe the figures. Please check and correct once more before the submission of revised manuscript (Now they are somewhat confused. Fig. 6 and 7 are examples. What really figure b and c imply? Direct description of figure a, b, c looks better to read).

The captions have been modified as requested. The implications of Panels (b) and (c) in each figure (Figures 6 and 7) are included at the end of Section 4.2.

Figure 6. Modelled and Pandora zenith-sky surface NO_2 vs. in situ NO_2. (a) shows the GEM-MACH modelled surface NO_2 data vs. in situ NO_2; (b) and (c) show the Pandora zenith-sky (ZS) surface NO_2 data vs. in situ NO_2. The Pandora ZS surface NO_2 data in (b) and (c) are derived using the hourly modelled conversion ratio and the monthly PSC-LUT, respectively. (d) to (f) are histograms corresponding to the data in (a) to (c). On each scatter plot, the red line is the linear fit with intercept set to 0 and the black line is the one-to-one line. The scatter plots are colour-coded by the normalized density of the points.

Figure 7. Modelled and Pandora direct-sun surface NO_2 vs. in situ NO_2. (a) shows the GEM-MACH modelled surface NO_2 data vs. in situ NO_2; (b) and (c) show the Pandora direct-sun (DS) surface NO_2 data vs. in situ NO_2. The Pandora DS surface NO_2 data in (b) and (c) are derived using the hourly modelled conversion ratio and the monthly PSC-LUT, respectively. (d) to (f) are histograms corresponding to the data in (a) to (c). On each scatter plot, the red line is the linear fit with intercept set to 0 and the black line is the one-to-one line. The scatter plots are colour-coded by the normalized density of the points.

The good consistency between $C_{pan\text{-}model}$, and $C_{pan\text{-}LUT}$ implies that two versions of Pandora surface NO_2 data can be delivered in the future, i.e., an off-line version that relies on hourly inputs from the model, and a near-real-time version that only needs a pre-calculated LUT.

Time period: Please clearly suggest the time period of each analysis (at least in each figure caption). I think each analysis has a different time period of analysis, which is a little complex to me. While I can accept this difference, the clear time information should be provided to help the readers' understanding.

Done. Captions of Figures 2, 4, and 6 to 10 are modified to include the period of each analysis.

Reference

ECCC: Canadian Environmental Sustainability Indicators: Air Quality. Environment and Climate Change Canada, ISBN: 978-0-660-06016-3, 2016.

Gao, R. S., Keim, E. R., Woodbridge, E. L., Ciciora, S. J., Proffitt, M. H., Thompson, T. L., Mclaughlin, R. J. and Fahey, D. W.: New photolysis system for NO_2 measurements in the lower stratosphere, J Geophys Res-Atmos, 99(D10), 20673–20681, doi:10.1029/94JD01521, 1994.

Gielen, C., Van Roozendael, M., Hendrick, F., Pinardi, G., Vlemmix, T., De Bock, V., De Backer, H., Fayt, C., Hermans, C., Gillotay, D. and Wang, P.: A simple and versatile cloud-screening method for MAX-DOAS retrievals, Atmos. Meas. Tech., 7, 3509–3527, doi:10.5194/amt-7-3509-2014, 2014.

Greenblatt, G. D., Orlando, J. J., Burkholder, J. B. and Ravishankara, A. R.: Absorption measurements of oxygen between 330 and 1140 nm, J. Geophys. Res., 95, 18577–18582, doi:10.1029/JD095iD11p18577, 1990.

Hudman, R. C., Jacob, D. J., Turquety, S., Leibensperger, E. M., Murray, L. T., Wu, S., Gilliland, A. B., Avery, M., Bertram, T. H., Brune, W., Cohen, R. C., Dibb, J. E., Flocke, F. M., Fried, A., Holloway, J., Neuman, J. A., Orville, R., Perring, A., Ren, X., Sachse, G. W., Singh, H. B., Swanson, A. and Wooldridge, P. J.: Surface and lightning sources of nitrogen oxides over the United States: Magnitudes, chemical evolution, and outflow, J Geophys Res-Atmos, 112(D12), doi:10.1029/2006JD007912, 2007.

Kelly, T. J., Spicer, C. W. and Ward, G. F.: An assessment of the luminol chemiluminescence technique for measurement of NO_2 in ambient air, Atmos. Environ., 24(9), 2397–2403, doi:10.1016/0960-1686(90)90332-H, 1990.

Lamsal, L. N., Martin, R. V., Donkelaar, A. van, Steinbacher, M., Celarier, E. A., Bucsela, E., Dunlea, E. J. and Pinto, J. P.: Ground-level nitrogen dioxide concentrations inferred from the satellite-borne Ozone Monitoring Instrument, J. Geophys. Res., 113(D16), doi:10.1029/2007JD009235, 2008.

Lee, C., Martin, R. V., Donkelaar, A. van, O’Byrne, G., Krotkov, N., Richter, A., Huey, L. G. and Holloway, J. S.: Retrieval of vertical columns of sulfur dioxide from SCIAMACHY and OMI: Air mass factor algorithm development, validation, and error analysis, J Geophys Res-Atmos, 114(D22), doi:10.1029/2009JD012123, 2009.

Maeda, Yasuaki., Aoki, Kenji. and Munemori, Makoto.: Chemiluminescence method for the determination of nitrogen dioxide, Anal. Chem., 52(2), 307–311, doi:10.1021/ac50052a022, 1980.

Martin, R. V., Chance, K., Jacob, D. J., Kurosu, T. P., Spurr, R. J. D., Bucsela, E., Gleason, J. F., Palmer, P. I., Bey, I., Fiore, A. M., Li, Q., Yantosca, R. M. and Koelemeijer, R. B. A.: An improved retrieval of tropospheric nitrogen dioxide from GOME, J. Geophys. Res., 107(D20), ACH 9-1-ACH 9-21, doi:10.1029/2001JD001027, 2002.

Martin, R. V., Sauvage, B., Folkins, I., Sioris, C. E., Boone, C., Bernath, P. and Ziemke, J.: Space-based constraints on the production of nitric oxide by lightning, J Geophys Res-Atmos, 112(D9), doi:10.1029/2006JD007831, 2007.

McClenny, W. A.: Recommended methods for ambient air monitoring of NO, NO_2, NO_y and individual NO_z species, Tech. rep., US Environmental Protection Agency, Traingle Park, NC 27711., 2000.

NRC: Rethinking the Ozone Problem in Urban and Regional Air Pollution, National Research Council, National Academy Press, Washington, D.C., 1992.

Park, R. J., Jacob, D. J., Field, B. D., Yantosca, R. M. and Chin, M.: Natural and transboundary pollution influences on sulfate-nitrate-ammonium aerosols in the United States: Implications for policy, J. Geophys. Res., 109(D15), doi:10.1029/2003JD004473, 2004.

Platt, U.: Differential optical absorption spectroscopy (DOAS), in Air Monitoring by Spectroscopic Techniques, pp. 27–84, John Wiley, New York., 1994.

Platt, U. and Stutz, J.: Differential Optical Absorption Spectroscopy: Principles and Applications, Springer, Germany, Berlin., 2008.

Ryerson, T. B., Williams, E. J. and Fehsenfeld, F. C.: An efficient photolysis system for fast-response NO_2 measurements, J. Geophys. Res., 105(D21), 26447–26461, doi:10.1029/2000JD900389, 2000.

Sauvage, B., Martin, R. V., Donkelaar, A. van, Liu, X., Chance, K., Jaeglé, L., Palmer, P. I., Wu, S. and Fu, T.-M.: Remote sensed and in situ constraints on processes affecting tropical tropospheric ozone, Atmos. Chem. Phys., 7(3), 815–838, doi:10.5194/acp-7-815-2007, 2007.

Thalman, R. and Volkamer, R.: Temperature dependent absorption cross-sections of O_2-O_2 collision pairs between 340 and 630 nm and at atmospherically relevant pressure, Phys. Chem. Chem. Phys., 15, 15371–15381, 2013.

Thornton, J. A., Wooldridge, P. J. and Cohen, R. C.: Atmospheric NO_2: In Situ Laser-Induced Fluorescence Detection at Parts per Trillion Mixing Ratios, Anal. Chem., 72(3), 528–539, doi:10.1021/ac9908905, 2000.

Wagner, T., Dix, B., Friedeburg, C. v, Frieß, U., Sanghavi, S., Sinreich, R. and Platt, U.: MAX-DOAS O_4 measurements: A new technique to derive information on atmospheric aerosols: Principles and information content, J. Geophys. Res., 109, D22205, doi:10.1029/2004jd004904, 2004.

Wagner, T., Apituley, A., Beirle, S., Dörner, S., Friess, U., Remmers, J. and Shaiganfar, R.: Cloud detection and classification based on MAX-DOAS observations, Atmos. Meas. Tech., 7, 1289–1320, doi:10.5194/amt-7-1289-2014, 2014.

Wagner, T., Beirle, S., Remmers, J., Shaiganfar, R. and Wang, Y.: Absolute calibration of the colour index and O_4 absorption derived from Multi AXis (MAX-)DOAS measurements and their application to a standardised cloud classification algorithm, Atmos. Meas. Tech., 9, 4803–4823, doi:10.5194/amt-9-4803-2016, 2016.

Wang, Y., Penning de Vries, M., Xie, P. H., Beirle, S., Dörner, S., Remmers, J., Li, A. and Wagner, T.: Cloud and aerosol classification for 2.5 years of MAX-DOAS observations in Wuxi (China) and comparison to independent data sets, Atmos. Meas. Tech., 8, 5133–5156, doi:10.5194/amt-8-5133-2015, 2015.

Wendel, G. J., Stedman, D. H., Cantrell, C. A. and Damrauer, Lenore.: Luminol-based nitrogen dioxide detector, Anal. Chem., 55(6), 937–940, doi:10.1021/ac00257a027, 1983.

Zhao, X., Bognar, K., Fioletov, V., Pazmino, A., Goutail, F., Millán, L., Manney, G., Adams, C. and Strong, K.: Assessing the impact of clouds on ground-based UV–visible total column ozone measurements in the high Arctic, Atmos. Meas. Tech., 12(4), 2463–2483, doi:10.5194/amt-12-2463-2019, 2019.